Eur. Phys. J. D **19**, 339–348 (2002)
DOI: 10.1140/epjd/e20020097

THE EUROPEAN PHYSICAL JOURNAL D
EDP Sciences

Magic numbers in heteroatom-containing carbon monocycles

G. Pascoli[1,a] and H. Lavendy[2]

[1] Faculté des Sciences, Département de Physique, 33 rue Saint-Leu, 80039 Amiens Cedex, France
[2] Laboratoire de Physique des Lasers, Atomes et Molcules, CNRS, CERLA, Université de Lille 1, bâtiment P5, 59655 Villeneuve d'Ascq Cedex, France

Received 13 December 2001 and Received in final form 26 February 2002

Abstract. Geometries, electronic structures and energetics of heteroatom-doped carbon clusters of the type C_nX^+ (X = B, Si; n = 9–15) have been investigated by means of the B3LYP (Becke 3-parameter-Lee-Yang-Parr) density functional method. The C_nB^+ (n = 9–15) cations are predicted to be planar monocycles while in the C_nSi^+ cations a linear form is favored for C_9Si^+ and structural transition from linear to planar ring-shape structure occurs at $n = 10$. Another difference between the two C_nB^+ and C_nSi^+ series is that in the C_nB^+ cations the boron atom is found to be incorporated into monocyclic structures whereas in the C_nSi^+ cations the silicon atom is bound to the outside of the carbon monocycle. More generally it is predicted that unlike first-row atoms such as B and N which can be easily networked into monocycles, second-row atoms such as Si, P and S are attached outside the carbon ring in capping position over two carbons. Incremental binding energy diagrams are also produced for the C_nB^+ and C_nSi^+ cations. It is shown that maxima of stability appear at $n = 10$ and 14 for the C_nB^+ cations in very close agreement with the experimental features. In contrast a clear theory-*versus*-experiment discrepancy has been evidenced in the C_nSi^+ cluster series where B3LYP results clearly contradict the experiments concerning the relative stability of these species. Possible explanations for this discrepancy are suggested.

PACS. 81.05.Uw Carbon, diamond, graphite – 36.40.-c Atomic and molecular clusters – 31.15.Ew Density-functional theory

1 Introduction

Whereas the smallest pure carbon clusters C_n are known to be linear chains with up to $n = 9$ [1,2], both theoretical studies and experiments suggest that conversion into a monocycle ring is energetically favored for large n [3–5]. As soon as $n \geq 10$, new chemical bond compensates for the increased strain-energy and the monocycle becomes lower in energy than the linear structure. A very interesting fact is that for pure carbon monocycles, in the range $10 \leq n \leq 30$, size-dependent oscillations in the dissociation energies are observed with a periodicity of four [3,6]. These oscillations which can be attributed to aromatic stabilization rapidly diminish with increasing cluster size [7].

Another important issue also concerns how heteroatoms belonging to the first and second rows of the periodic table can affect the geometry of the carbon clusters. Experimental data are especially available for boron-doped and silicon-doped carbon compounds owing to their technological interest [8,9]. Unfortunately, the experimental results are generally obtained for cluster series in the ionic state (as due to the experimental devices, that is for instance, laser vaporization and injected ion drift techniques) and it is implicitly hypothesized that the charge does not strongly influence the geometry and stability when going from the ionic to the neutral species. For neutral species, the best approach is still to perform theoretical studies where calculations can simultaneously be conducted for both ions and neutrals. On the theoretical side, however, two major problems are encountered when applying usual *ab initio* methods to pure carbon or mixed heteroatom-carbon systems of medium and large sizes, namely CPU time and disk space. Searching for an alternative, density functional theory has recently generated a lot of interest [10–14]. Among the gradient corrected functionals, the more sophisticated B3LYP method has been extremely successful in reproducing many properties such as, for instance, the geometries, rotational constants, vibrational frequencies [11–13], the adiabatic electronic affinities [14] and vibrational circular dichroism spectra [10] of a number of small and medium-sized molecules.

Nevertheless, for pure carbon clusters, it has been shown that B3LYP seems less dependable for the evaluation of the relative energetics than other *ab initio* methods such as CCSD(T) [11]. Thus CCSD(T) computations have to be carried out on geometries calculated at B3LYP level for any classes of molecules in order to test

[a] e-mail: pascoli@u-picardie.fr

Table 1. Binding energies (in eV) calculated from B3LYP/6-311G* reference geometries and number of π electrons in C_nB^+ ($n = 9$–15) cations. Electronic states are also given.

species	structure	electronic state	binding energy		number of π electrons	
			B3LYP	CCSD(T)	regular	in-plane
C_9B^+	cyclic	$^1A_1$	58.21	53.49	9	9
		$^3B_1$	+0.22	−0.16	10	8
$C_{10}B^+$	cyclic	$^1A_1$	66.52	61.34	10	10
		$^3B_2$	−1.85	−2.21	10	10
$C_{11}B^+$	cyclic	$^1A_1$	72.12	66.25	10	12
		$^3B_1$	−0.06	−0.45	11	11
$C_{12}B^+$	cyclic	$^1A_1$	78.78	70.24	12	12
		$^3A_2$	−0.90	−0.67	13	11
$C_{13}B^+$	cyclic	$^1A_1$	85.23	78.30	12	14
		$^3B_2$	−0.50	−0.81	14	12
$C_{14}B^+$	cyclic	$^1A_1$	93.02		14	14
		$^3B_1$	−2.21		15	13
$C_{15}B^+$	cyclic	$^1A_1$	98.06		15	15
		$^3B_1$	+0.58		16	14

more specifically the triplet/singlet, quadruplet/doublet and linear/cyclic energetical orderings.

The present study is devoted to the cations C_nX^+ (X = B, N, O, Al, Si, P, S) and we shall focus on the low-energy cyclic geometries in the range $n = 9$–15. In particular, a special attention is delivered on C_nB^+ and C_nSi^+ cations. Like for pure carbon clusters, series of these heteroatomic systems exhibit prominent magic peaks and fourfold periodicity in stability. The role of both the charge and the size of the heteroatom is then discussed.

2 Methods

The quantum chemical computations were conducted with the GAUSSIAN 94 computational package [15] implemented on a IBM-SP3 computer.

The Pople's 6-311G* (contracted $3s3p1d$ for boron and carbon, $6s5p1d$ for silicon) basis set has been employed [16]. This basis exhibits the needed flexibility and is small enough in size to be applicable to medium-sized clusters. The 6-311G* basis was found to supply results (geometries and energy separations) of nearly the same quality as those obtained with more accurate basis such as cc-pVTZ in the case of heteroatom-containing carbon clusters [17]. The optimization of structures has been carried out with the B3LYP hybrid density functional which is a combination of the three parameter Becke exchange functional [18] with the Lee-Yang-Parr non local correlation functional [19]. Even though extremely time-demanding, the coupled cluster method including all single and double excitations and a non-iterative perturbational correction to account for connected triple excitations (CCSD(T) [20,21] has been also used in order to test the B3LYP energetics. Excluding the fact that its accuracy can be limited by the basis set, the latter method yields the best results provided non-dynamical correlation effects do not become pathological [22]. On the other hand, a related advantage of the CCSD(T) approach over other methods such as, for instance, the CISD method is its size-consistency. Size-consistency (*i.e.* linear relationship between cluster size and energy) is important whenever calculations on molecules of different sizes are to be compared as in the present study.

Each equilibrium geometry was characterized by analysis of the harmonic vibrational frequencies, obtained from analytic second-order derivative techniques. This enables us to assess the nature of the stationary points, to verify that they correspond to true minima on the potential energy surface (no imaginary frequency) and also to estimate the zero-point energy (ZPE) correction. For the sake of space, these results are not listed but are available upon request.

3 The cations C_nB^+

The lowest-energy structure for the C_nB^+ ($n = 9$–15) cations is predicted to be the monocyclic arrangement of nuclei with the boron atom incorporated into the carbon cycle. The electronic state is dominantly the singlet $^1A_1$ along the series, except in the case of C_9B^+ and $C_{15}B^+$ where the triplet $^3B_1$ is predicted the most stable one at B3LYP level, with energy separations of the order of 5.0 kcal mol^{-1} (C_9B^+) and 13.4 kcal mol^{-1} ($C_{15}B^+$) (Tab. 1). We can however notice that for C_9B^+ the singlet is eventually more stable than the triplet at the CCSD(T) level (by 3.7 kcal mol^{-1}). The triplet-singlet energy difference is also found to be very weak in $C_{11}B^+$, of the order of 1 kcal mol^{-1} at B3LYP level, but the energetic ordering is, this time, respected at CCSD(T) level (Tab. 1). In all

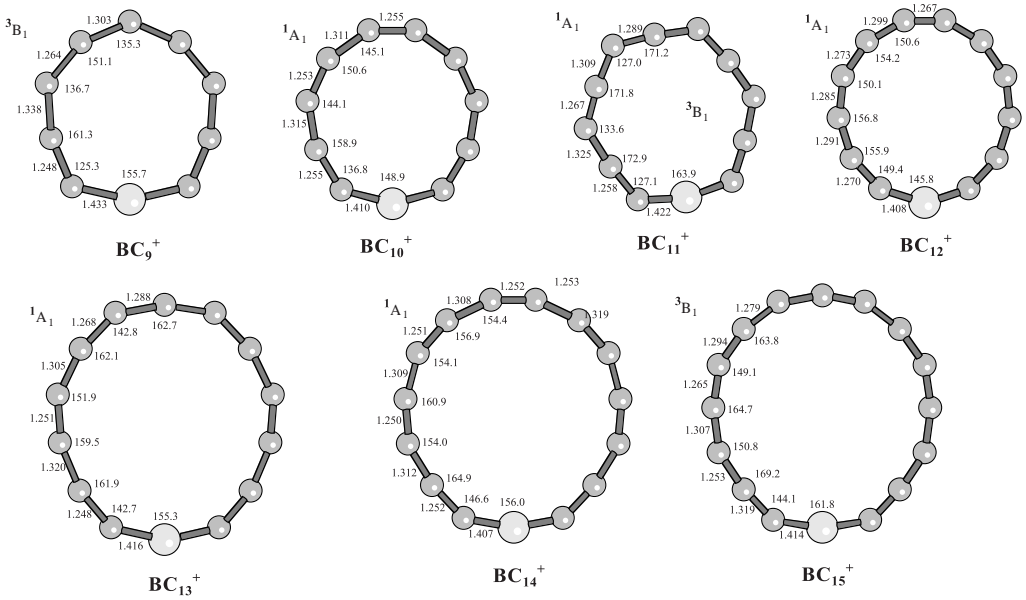

Fig. 1. Ground state geometries of C_nB^+ (n = 9–15) cations. Distances are in Å and angles in degrees. The B3LYP total energy (in Hartree) is given under each structure.

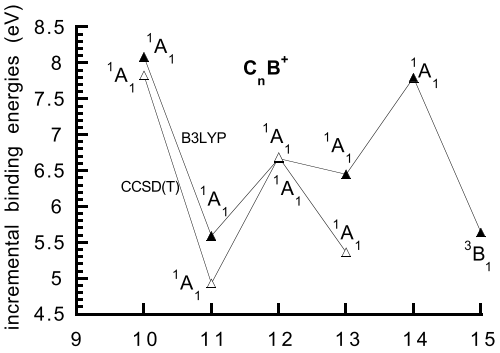

Fig. 2. Incremental binding energies of C_nB^+ (n = 9–15) cations.

these compounds the B–C distance is invariably of the order of 1.43 Å and C–C distances are between 1.25 Å and 1.35 Å (Fig. 1). Typical alternations of long ∼1.30–1.32 Å and short ∼1.25–1.27 Å C–C bonds are also conspicuous conferring to these cumulene-type molecules some polyacetylenic character. Most important is the fourfold periodicity in stability predicted from the incremental binding energy diagram as usually arising in closed-ring systems (Fig. 2). The incremental binding energy is the change in binding energy accompanying the following process

$$C_nX^+ \rightarrow C_{n-1}X^+ + C$$

where X indicates the heteroatom. This quantity gauges the relative stability of heteroatom-doped carbon clusters [23] is reported in Figure 2 (ZPE corrections, when included, tend to systematically decrease the estimated incremental binding energies by about 0.1–0.2 eV). This figure shows that maxima of stability are obtained for a number of carbon atoms equal to 10 and 14 both at B3LYP and CCSD(T) levels of theory, that is for $n = 4k + 2$ with k an integer. This result is consistent with the mass-spectrometry experiments of Becker and Dietze [24] and Kimura *et al.* [8]. In the framework of the molecular orbital theory, [25], we can distinguish two patterns of $2p_\pi$ orbitals, the regular system, perpendicular to the plane of the molecule, and the in-plane system composed of p_π orbitals radially oriented in the plane of the ring (the dangling bonds surrounding the molecule). Maxima of stability occur for the molecule when the number of regular and in-plane π electrons are both equal to magic (aromatic) numbers $4k + 2$ that is, in our study, 10 and 14 (Tab. 1). In contrast, a lower stability arises for $C_{12}B^+$, the latter molecule being doubly anti-aromatic (each of the regular and in-plane π systems accommodating $4k$ electrons). In fact, the regular and in-plane systems are not equivalent. The overlap of regular p_π orbitals is much more pronounced than the overlap of in-plane p_π orbitals. Consequently the regular system plays the most important role in the stability as we shall see for the C_nSi^+ cations.

4 The cations C_nSi^+

A general rule is that along the C_nSi^+ cluster series, the low-lying quadruplet state is always located higher in energy than the doublet ground state (with average doublet-quadruplet energy separation of the order of 30 kcal mol^{-1}) Then, in the following, we shall only concentrate the discussion on the doublets.

The lowest-energy isomer of C_9Si^+ is predicted to be the linear arrangement of nuclei in the $^2\Pi$ electronic state. The cyclic form with capping Si lies at 10.4 kcal mol^{-1} and 1.0 kcal mol^{-1} above the linear ground state, respectively at B3LYP and CCSD(T) levels (Tab. 2). For $n = 10$ and larger clusters, the Si-capped structure definitely becomes the most stable one. The monocyclic isomer with

Table 2. Binding energies (in eV) calculated from B3LYP/6-311G* reference geometries and number of π electrons in C_nSi^+ ($n = 9$–15) cations. Electronic states are also given.

species	structure	electronic state	binding energy		number of π electrons	
			B3LYP	CCSD(T)	regular	in-plane
C_9Si^+	linear	$^2\Pi$	56.53	51.91	$(4 \times 4)+1$	
	cyclic	$^2B_1$	−0.45	−0.04	10	7
$C_{10}Si^+$	cyclic	$^2B_2$	63.48	58.95	10	9
$C_{11}Si^+$	cyclic	$^2B_1$	70.02	64.56	11	10
$C_{12}Si^+$	cyclic	$^2A_2$	75.56	69.89	13	10
$C_{13}Si^+$	cyclic	$^2A_2$	83.02	76.42	14	11
$C_{14}Si^+$	cyclic	$^2B_2$	90.01		14	13
$C_{15}Si^+$	cyclic	$^2B_1$	96.46		15	14

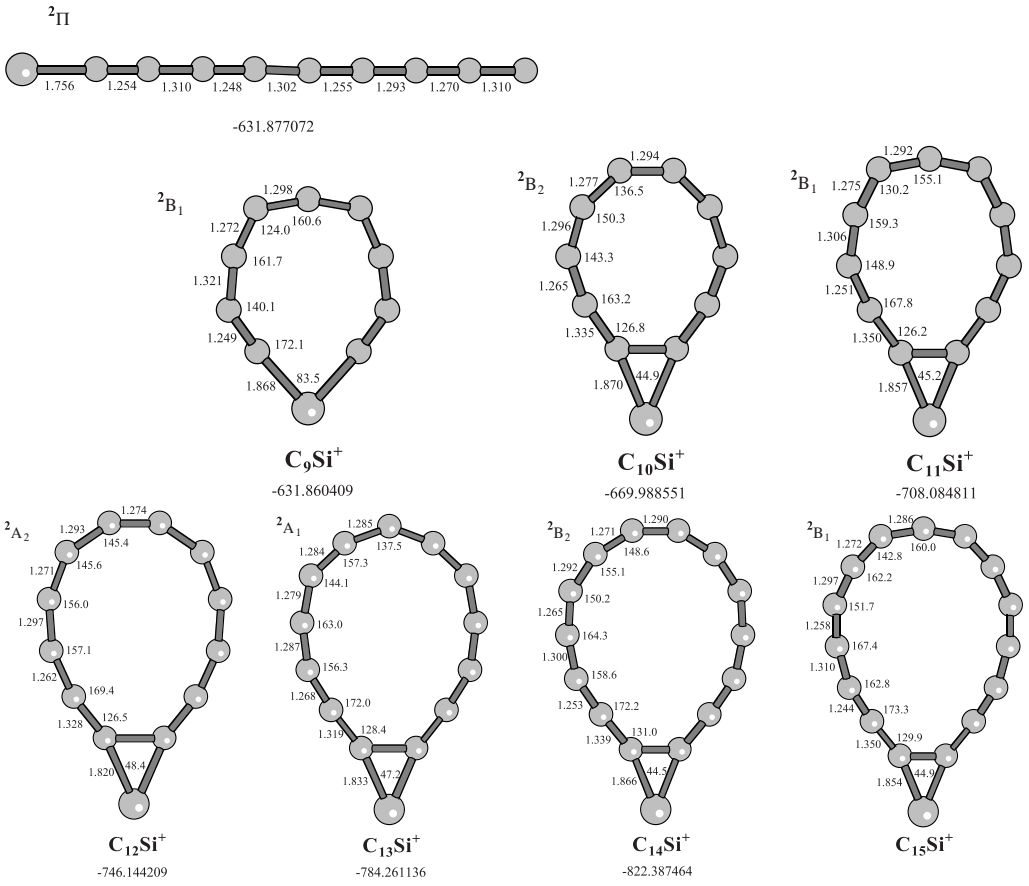

Fig. 3. Equilibrium geometries of energetically low-lying structures of C_9Si^+ and ground state geometries of C_nSi^+ ($n = 10$–15) cations. Distances are in Å and angles in degrees.

Si directly incorporated into the C_n ring is, in all cases, located higher in energy above the Si-capped carbon ring with energy separations in the range 20–40 kcal mol^{-1}. On the other hand, the frequencies are not all real and consequently the monocycle eventually corresponds to a saddle point on the potential energy surface. Thus in the following, the discussion concerns only the ground state geometry (Si-capped C_n structure). In this one, the C_n sub-system, with normal double C–C bonds ∼1.29–1.31 Å alternating with strong double C–C bonds ∼1.25–1.27 Å can be regarded as a cumulenic ring with some surimposed polyacetylenic character. As for the capping Si, the Si–C bond lengths are found to be in the range 1.75–1.85 Å typical of moderately weak Si–C single bonds. The C–Si–C angle is predicted to be very acute, in the range 45–50° along the cluster series. Let us however notice that the silicon-bridged C–C bond with length ∼1.45–1.50 Å is somewhat elongated for a normal double C–C bond which markedly distorts the cumulenic C_n ring. Some traits of this archetypical structure (neutral carbon monocycle and positive capping Si) are already present in the C_3Si^+ rhomboidal cation where the Si–C distances are ∼1.94 Å and the C–Si–C angle ∼46.1° at B3LYP level of theory [26]. The relative stabilities along the C_nSi^+

species	structure	electronic state	binding energy B3LYP	number of π electrons regular	in-plane
C_9Si	linear	$^3\Sigma^-$	56.17	$(4\times4)+2$	
	cyclic	$^1A_1$	+0.10	10	8
$C_{10}Si$	cyclic	$^1A_1$	63.33	10	10
$C_{11}Si$	cyclic	$^1A_1$	68.86	11	11
		$^3B_1$	−0.03	12	10
$C_{12}Si$	cyclic	$^1A_1$	75.66	12	12
$C_{13}Si$	cyclic	$^1A_1$	82.52	14	12
$C_{14}Si$	cyclic	$^1A_1$	89.50	14	14
$C_{15}Si$	cyclic	$^1A_1$	94.93	14	16

Table 3. Binding energies (in eV) calculated from B3LYP/6-311G* reference geometries and number of π electrons in C_nSi (n = 9–15) clusters. Electronic states are also given.

species	structure	symmetry	multiplicity	binding energy B3LYP	CCSD(T)	number of π electrons regular	in-plane
C_9	linear	$D_{\infty h}$	1	51.64	47.36	4×4	
	cyclic	C_{2V}	1	−0.91	−0.45	10	8
C_9^+	linear	$D_{\infty h}$	2	53.63	49.04	$(4\times3)+3$	
	cyclic	C_{2V}	2	+0.18	+0.50	10	7
C_{10}	cyclic	D_{5h}	1	59.78	55.42	10	10
C_{10}^+	cyclic	C_{2V}	2	62.01	57.29	10	9
C_{11}	cyclic	C_{2V}	1	65.02	60.18	10	12
C_{11}^+	cyclic	C_{2V}	2	69.06	63.28	11	10
C_{12}	cyclic	C_{6h}	1	71.43	64.89	12	12
C_{12}^+	cyclic	D_{6h}	2	74.98	68.02	12	11
C_{13}	cyclic	C_{2V}	1	77.88	71.82	14	12
C_{13}^+	cyclic	D_{2V}	2	81.56	74.60	14	11
C_{14}	cyclic	D_{7h}	1	86.11		14	14
C_{14}^+	cyclic	C_{2V}	2	91.31	82.22	14	13
C_{15}	cyclic	C_{2V}	1	91.37		14	16
C_{15}^+	cyclic	C_{2V}	2	95.79		15	14

Table 4. Binding energies (in eV) calculated from B3LYP/6-311G* reference geometries and number of π electrons in neutral C_n and related cations C_n^+ (n = 9–15).

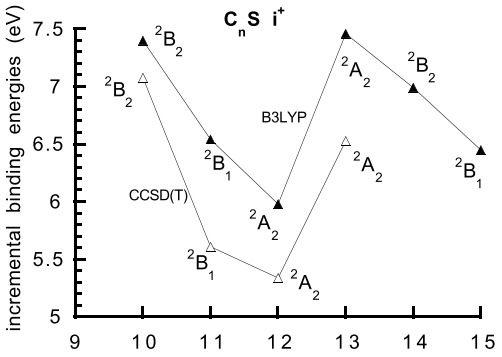

Fig. 4. Incremental binding energies of C_nSi^+ (n = 9–15) cations.

(n = 9–15) cation series can again be analyzed with help of the incremental energy diagram reproduced in Figure 4 (ZPE corrections, when included, tend to systematically decrease the incremental binding energies by about 0.1–0.2 eV). Maxima of stability occur at $n = 10$ and 14. From Table 2, we can see that the corresponding clusters possess a number of regular electrons equal to a magic number, that is $4k + 2$ with $k = 2$ and 3 in analogy with Hückel's rule for aromatic hydrocarbons [25].

The magic number 14 appears also for $C_{13}Si^+$ and the stability of this species is high (Fig. 4). However and surprisingly enough, these results are not confirmed by the experiments [8,27]. In mass spectra experiments, Kimura *et al.* [8] found prominent peaks in the intensity distribution of C_nSi^+ clusters at n = 11, 15 instead of n = 10, 14 as like in the present study (let us however notice the existence of a short peak at $n = 18$ and not 19 in their experimental curve). B3LYP/6-311G* energetics could yet be questioned but the CCSD(T) approach gives very similar results. In order to understand the origin of this discrepancy, we have calculated the incremental binding energies of the corresponding neutrals which are displayed in Figure 5. Peaks are seen at n = 10 and 14 (Fig. 6) corresponding to magic numbers $4k + 2$ with $k = 2$ and 3 in both regular and in-plane π electron systems (Tab. 3). Eventually, given the important role played by the C_n ring sub-system present in these structures, we have also calculated the incremental binding energies for neutral and cationic pure carbon monocycles (Figs. 7, 8 and Tab. 4). Once again, prominent peaks are seen at n = 10 and 14

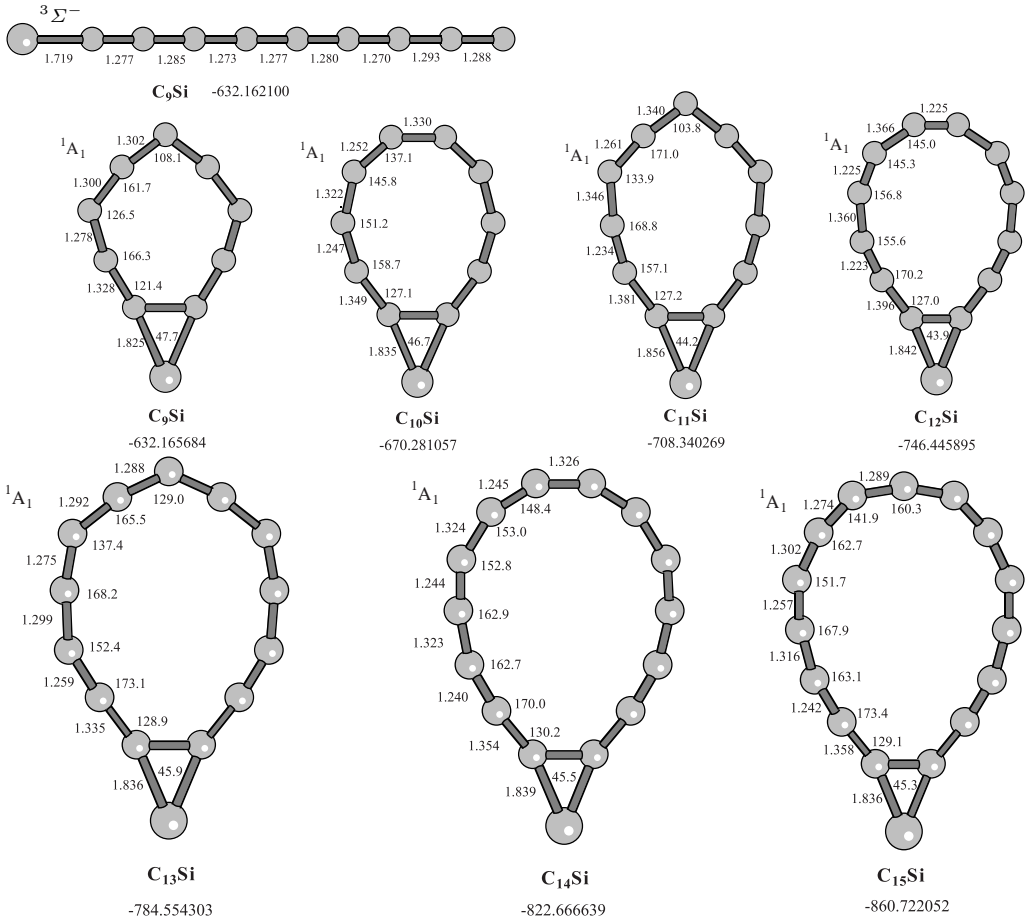

Fig. 5. Equilibrium geometries of energetically low-lying structures of neutral C_9Si and ground state geometries of neutral C_nSi ($n = 10$–15) clusters. Distances are in Å and angles in degrees. The B3LYP total energy (in hartree) is given under each structure.

for both cations and neutrals (Fig. 8). In the neutral C_n series, the C_{4k+2} ($k = 2$, 3) clusters are cumulenic rings with $D_{(2k+1)h}$ symmetry (Fig. 7). These clusters are doubly aromatic (Tab. 4). In contrast C_{12} is found to be a polyacetylenic ring with double and strong double C–C bond alternation resulting in a C_{6h} symmetry. C_{12} is antiaromatic in both regular and in-plane π electron systems. All these results are incidentally consistent with conclusions made by other authors on C_{2n} neutral clusters [11]. Globally, going from the neutrals to the cations, one electron is removed from the in-plane π electron system. But the stability being essentially governed by the regular π electron system (maximum overlap of π orbitals), the relative stabilities of C_n clusters, both in their neutral or cationic forms, remain nearly unchanged.

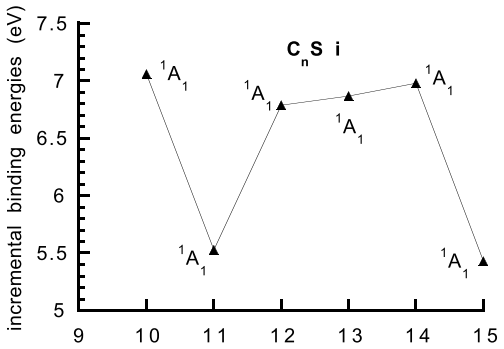

Fig. 6. Incremental binding energies of neutrals C_nSi ($n = 9$–15).

The problem can still be analyzed from another point of view. We note that the equilibrium geometry of the C_nSi ($10 \leq n \leq 15$) clusters is permanently cyclic with C_{2V} symmetry in both neutral and cationic forms. This suggests that the removal of one electron does not drastically modify the topology of these species. On the basis of this crude statement, the ionization energies of the C_nSi molecules have been first identified to the adiabatic ionization potentials (AIP) computed by differences between the total energies of the optimized cations and the total energies of the optimized neutrals (Fig. 9). Small variations in bond lengths and angles are however perceptible and in C_9Si and $C_{11}Si$, structural rearrangements after ionization are relatively important (Figs. 3 and 5). So it appears more relevant in these cases to eventually use the vertical ionization potentials (VIP), that is the change in total energy going from the neutral in its ground state to

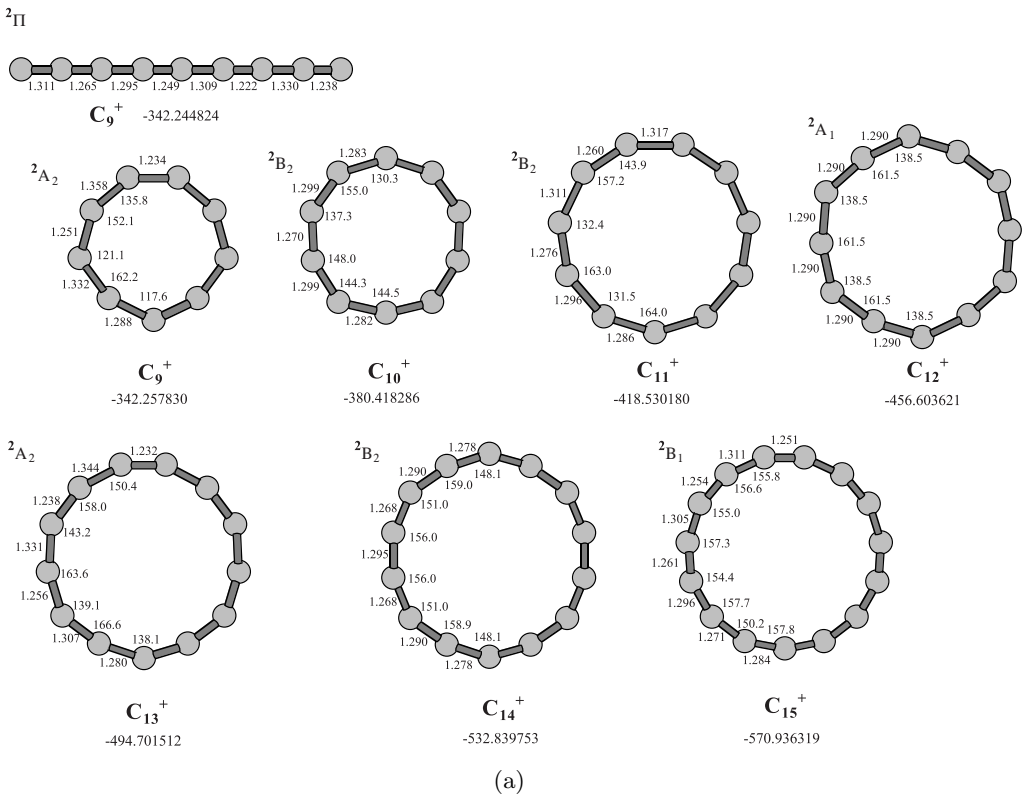

Fig. 7. Equilibrium geometries of energetically low-lying structures of C_9 and C_9^+ and ground state geometries of neutrals C_n and related cations C_n^+ (n = 10–15). Distances are in Å and angles in degrees. The B3LYP total energy (in hartree) is given under each structure.

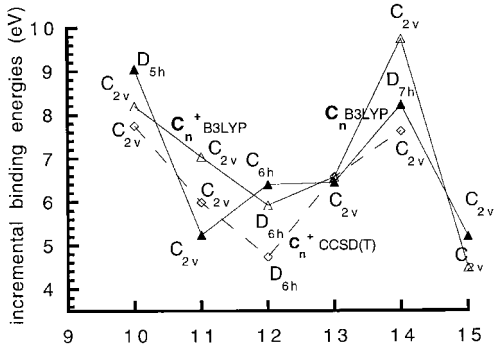

Fig. 8. Incremental binding energies of C_n and C_n^+ ($n = 9$–15).

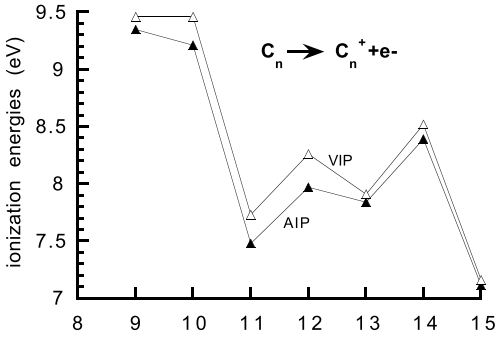

Fig. 10. Ionization potentials of neutral C_n clusters. AIP, adiabatic ionization potential; VIP, vertical ionization potential.

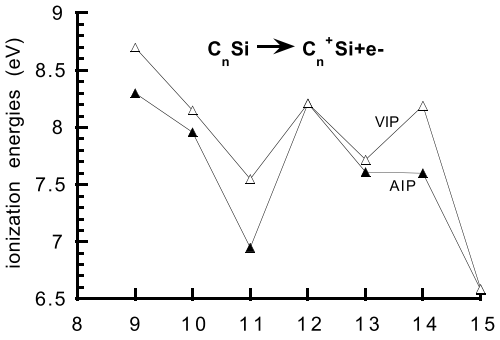

Fig. 9. Ionization potentials of neutrals C_nSi. AIP, adiabatic ionization potential; VIP, vertical ionization potential.

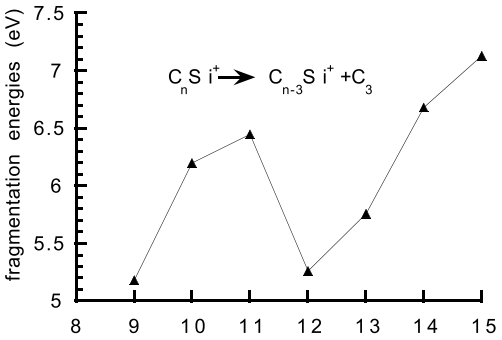

Fig. 11. Fragmentation energies of C_nSi^+ cations.

the ionized structure before relaxation, *i.e.* without change in the position of the ionic cores (as the ionization timescale precludes any structural rearrangement during the process of ejection of the electron). The corresponding results are also reported in Figure 9. Simple examination of this figure immediately reveals that the ionization energy of $C_{10}Si$ is higher than that of $C_{11}Si$ and likewise when comparing $C_{14}Si$ against $C_{15}Si$. It can thus be conjectured that, if, in some experiment, C_nSi molecules are produced and then analyzed in mass spectra after ionization, $C_{11}Si^+$ could then appear more abundant than $C_{10}Si^+$ (likewise for $C_{15}Si^+$ against $C_{14}Si^+$), the shift in dominance arising from the ionization process itself, the latter one overcompensating the fact that clusters with high stability are indeed invariably $C_{10}Si$ and $C_{14}Si$ (in both neutral and cationic forms). Kimura *et al.* [8] justify their results, that is maximum of intensity in mass spectra at $n = 11$ and 15 for C_nSi^+ clusters by simply invoking the filling of π orbitals. Unfortunately, the latter authors do not state specifically which of the two π electron systems, regular or in-plane, is concerned in their reasoning. Furthermore, their intensity distribution for the C_nSi^+ cations can or cannot reflect the relative stability of individual clusters, given that the ionic to neutral abundance ratio is unknown in reference [8] (the neutrals are indeed, as usually, not observed in these experiments and the ionic to neutral abundance ratio is linked to the ionization cross-section which in turn strongly depends on the experimental set-up). Such a conclusion already occurs in pure carbon clusters as attested by Figure 10 (to be compared to the experimental curves displayed in Fig. 8 in Ref. [6]). Similar difficulties in the interpretation of the abundance graphs when comparing theory and experiment (or high energy and low energy ionization experiments) also appear in other fields of cluster science [28]. Relative stabilities of clusters can likewise be evaluated within the framework of the fragmentation patterns. Major fragmentation channel is loss of C_3 neutral (Fig. 11). This figure again displays a fourfold periodicity. But we can verify this time that $C_{10}Si^+$ and $C_{11}Si^+$ exhibit quite comparable behaviour against dissociation by C_3 loss (likewise for $C_{14}Si^+$ and $C_{15}Si^+$) and consequently the latter process plays a lesser role than ionization with regard to the relative abundances of $C_{10}Si^+$ *versus* $C_{11}Si^+$ ($C_{14}Si^+$ *versus* $C_{15}Si^+$). Eventually, another point is worth mentioning as for the interpretation of the incremental binding energy diagrams. Up to now, we have focused our attention on the energetics at 0 K. However temperature could influence the stabilities and modify the binding energies. We have considered this possibility by computing the latter quantities in the temperature range 500–1 000 K. Our analysis clearly shows that temperatures smaller than 1 000 K have essentially no influence on the diagrams (maximal change in the estimated incremental binding energies ∼0.2 eV). Therefore the conclusion drawn at 0 K should apply equally well to temperatures reaching up 1 000 K (in most experiments, clusters are quickly cooled below this temperature prior mass analysis).

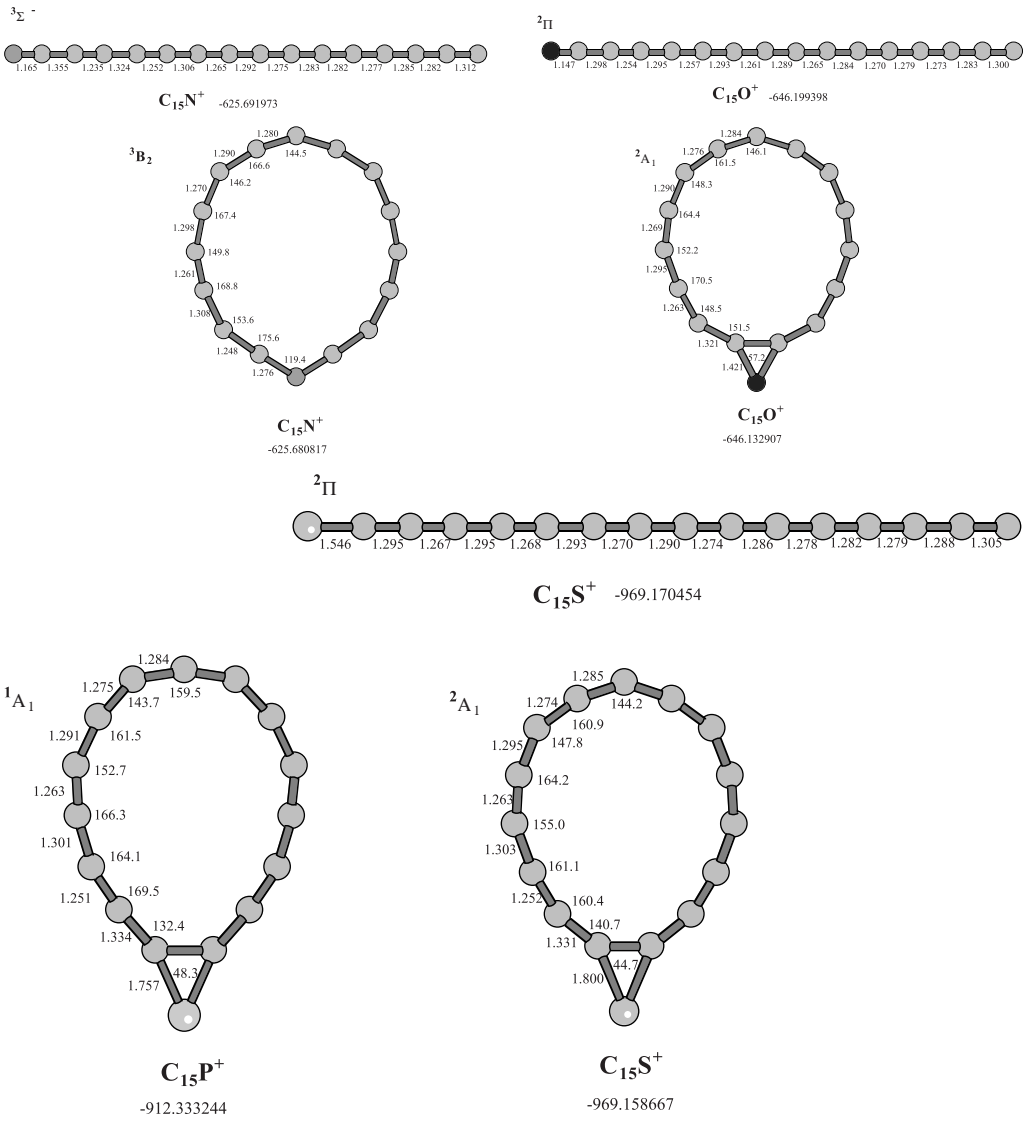

Fig. 12. Equilibrium geometries of $C_{15}X^+$ (X = N, O, Al, P, S) cations. Distances are in Å and angles in degrees. The B3LYP total energy (in hartree) is indicated under each structure. When the ground state geometry is linear, the low-lying cyclic structure is also supplied.

5 The cations C_nX^+ (X = N, O, Al, P, S)

The conclusions of the two preceding sections for boron-doped and silico-doped carbon clusters are easily transposable on other heteroatom-containing carbon clusters belonging respectively to the first and second rows of the periodic table, but with a few changes however given the fact that the electronic structure of some heteroatoms imposes to the cluster to remain linear even for large value of n. We shall choose for comparison the $C_{15}X^+$ cation (Fig. 12).

The lowest-energy isomer of the nitrogen-doped carbon cation $C_{15}N^+$ is found to be the linear triplet ($^3\Sigma^-$) with the nitrogen atom in terminal position. The C–N bond length is short, of the order of 1.17 Å comparable to a normal triple C–N bond. The monocycle with N in insertion is predicted less stable than the linear structure although by only 7.0 kcal mol^{-1}. In contrast, $C_{15}O^+$ is found to be clearly linear in the $^2\Pi$ electronic ground state. Both the cyclic structures accomodating the oxygen atom either inside or outside the carbon ring are local minima but not competitive in energy given they are located respectively at 41.7 and 47.6 kcal mol^{-1} above the linear ground state. Another interesting, but quite distinct situation, concerns $C_{15}Al^+$ for which we predict this time a carbon ring with exocyclic Al as lowest-energy isomer. But the corresponding monocycle with Al directly networked into the carbon ring ($^3B_1$) is lying only 2.5 kcal mol^{-1} higher in energy (0.8 kcal mol^{-1} after inclusion of the ZPE correction). Consequently, these two cyclic species could simultaneously coexist in equal ratio in mass spectrometry experiments for the $C_{15}Al^+$ cation. This, in turn, suggests that the incorporation of a large size atom into a carbon ring is feasible in some cases without producing significant strain for the ring structure. In fact the atomic

size does not appear a criterion good enough to ascertain whether the heteroatom can be networked into the carbon ring. Nevertheless, for other heteroatoms belonging to the second row of the periodic table, we find that the cyclic structure with exohedral heteroatom is favored over the monocycle, by of the order of 9.4 kcal mol^{-1} in the case of $C_{15}P^+$ and 55.1 kcal mol^{-1} in $C_{15}Si^+$. Furthermore, vibrational frequency analysis reveals that for $C_{15}Si^+$ the monocyclic geometry is not a local minimum on the potential energy surface (one big imaginary frequency of 459i). Eventually, and very similarly to what is observed for its first row analog $C_{15}O^+$, the lowest-energy isomer of $C_{15}S^+$ is indeed the linear $^2\Pi$; but, in contrast to $C_{15}O^+$, the cyclic structure with exohedral S is just 7.1 kcal mol^{-1} higher in energy than the linear form. We can conclude that, very possibly, both the linear and cyclic states could be accessible to experimental detection for the latter compound.

As final remark, it is worthy to note that for all the species studied, in the cyclic isomer with exohedral heteroatom, the C–C distance bridged by the heteroatom is invariably of the order of 1.42–1.43 Å and the carbon ring is roughly cumulenic with some polyacetylenic character.

6 Conclusions

For the class of molecules under consideration, *i.e.* carbon clusters with one heteroatom belonging to either the first or the second row of the periodic table, it appears that B3LYP is an efficient tool for predicting accurate equilibrium geometries with high cost-to-benefit ratio. We can also infer with some confidence that this method completed with CCSD(T) calculations can help the experimentalists using mass spectrometry. Especially the intensity distribution in mass spectra for heteroatom-doped carbon clusters can generally be rationalized in qualitative terms based on filling of π orbitals of individual clusters, even though some discrepancies (+1 shift in the abundance) between theory and experiment have been neverthelesss clearly evidenced in silicon-doped carbon clusters. On the other hand, in a few compounds, competition is shown to be existing between distinct isomers, a definite situation which could yet introduce further intricacy in the analysis of the experimental spectra.

The Laboratoire de Physique des Lasers, Atomes et Molécules is "Unité Mixte de Recherche de l'Université de Lille 1 et du CNRS n° 8523", the Centre d'Études et de Recherches Lasers et Applications (CERLA) is supported by the Ministère chargé de la Recherche, the Région Nord-Pas de Calais and the Fonds Européen de Développement Économique des Régions. The computations have been carried out at the CRI (Centre de Ressources Informatiques) on the IBM-SP3 which is supported by the programme de calcul intensif of the Ministère de la Recherche, the Région Nord Pas-de-Calais and the Fonds Européen de Développement Régional: FEDER.

References

1. K. Ragavachari, J.S. Binkley, J. Chem. Phys. **87**, 2191 (1987).
2. A. van Orden, H.J. Huang, E.W. Kuo, R.J. Saykally, J. Chem. Phys. **98**, 6678 (1993).
3. G. von Helden, M.-T. Hsu, N.G. Goth, M.T. Bowers, J. Phys. Chem. **97**, 8182 (1993).
4. S.W. Mc Elvaney, B.I. Dunlop, A. O'Keefe, J. Chem. Phys. **86**, 715 (1987).
5. G. von Helden, M.T. Hsu, P.R. Kemper, M.T. Bowers, J. Chem. phys. **95**, 3835 (1991).
6. W. Weltner Jr, R.J. van Zee, Chem. Rev. **89**, 1713 (1989), and references therein.
7. J.M. Hunter, J.L. Fye, E.J. Roskamp, H.F. Jarrold, in *Molecules and Grains in space*, edited by I. Nenner (IAP Conference Proceedings 312, New York, 1994), p. 571.
8. T. Kimura, T. Sugai, H. Shinohara, Chem. Phys. Lett. **256**, 269 (1996).
9. J.L. Fye, M.F. Jarrold, J. Chem. Phys. **101**, 1836 (1997).
10. P.J. Stephens, F.J. Devkin, C.F. Chabolowski, M.J. Frisch, J. Phys. Chem. Lett. **98**, 11623 (1994).
11. M.L.J. Martin, J. El-Yazal, J.P. François, Chem. Phys. Lett. **242**, 570 (1995).
12. J.D. Presilla-Marquez, C.M.L. Rittby, R.M. Graham, J. Chem. Phys. **106**, 8367 (1997).
13. G. Pascoli, H. Lavendy, Int. J. Mass Spectrom. Ion Proc. **181**, 11 (1998).
14. S.T. Brown, J.C. Rienstra-Kiracofe, H.F. Schaefer III, J. Phys. Chem. A **103**, 4065 (1999).
15. M.J. Frisch, G.W. Trucks, H.B. Schlegel, P.M.W. Gill, B.G. Johnson, M.A. Robb, J.R. Cheeseman, T. Keith, G.A. Petersson, J.A. Montgomery, K. Raghavachari, M.A. Al-Laham, V.G. Zakrzewski, J.V. Ortiz, J.B. Foresman, J. Ciolowski, B.B. Stefanov, A. Nanayakkara, M. Challacombe, C.Y. Peng, P.Y. Ayala, W. Chen, M.W. Wong, J.L. Andres, E.S. Replogle, R. Gomperts, R.L. Martin, D.J. Fox, J.S. Binkley, D.J. Defrees, J. Baker, J.P. Stewart, M. Head-gordon, C. Gonzalez, J.A. Pople, *Gaussian 94, Revision C.3* (Gaussian, Inc., Pittsburgh P.A. 1995).
16. R. Krishnan, J.S. Binkley, R. Seeger, J. Pople, J. Chem. Phys. **72**, 650 (1980).
17. G. Pascoli, H. Lavendy, Int. J. Mass Spectrom. Ion Proc. **206**, 153 (2001).
18. A.D. Becke, J. Chem. Phys. **98**, 5648 (1993).
19. C. Lee, W. Yang, R.G. Parr, Phys. Rev. B **37**, 785 (1988).
20. J.A. Pople, M. Head-Gordon, K. Raghavachari, J. Chem. Phys. **87**, 5968 (1987).
21. K. Raghavachari, G.W. Trucks, J.A. Pople, M. Head-Gordon, Chem. Phys. Lett. **157**, 479 (1989).
22. G.E. Scuseria, T.J. Lee, J. Chem. Phys. **93**, 585 (1990).
23. S. Fliszár, *Charge Distribution and Chemical Effects* (Springer Verlag, New York, 1983).
24. S. Becker, H.J. Dietze, Int. J. Mass Spectrom. Ion Proc. **82**, 287 (1988).
25. K.S. Spitzer, E.J. Clementi, Am. Chem. Soc. **81**, 4477 (1959).
26. H. Lavendy, J.M. Robbe, J.P. Flament, G. Pascoli, J. Phys. Chem. **94**, 1779 (1997).
27. A. Benninghoven, S. Sichtermann, S. Storp, Thin Solid Films **28**, 59 (1975).
28. W.A. De Heer, Rev. Mod. Phys. **65**, 611 (1993), and papers of Brechignac *et al.* quoted therein.